ICSV19
Vilnius, Lithuania
July 08-12, 2012

NONLINEAR PHENOMENA IN THERMOACOUSTICS: A COMPARISON BETWEEN SINGLE-MODE AND MULTI-MODE METHODS

Karthik Kashinath and Matthew P. Juniper

Dept. of Engineering, Cambridge University, Cambridge - CB21PZ, U.K.,
e-mail: kk377@cam.ac.uk

Santosh Hemchandra

Dept. of Aerospace Engineering, Indian Institute of Science, Bangalore-560012, India

Nonlinear analysis of thermoacoustic instability is essential for prediction of frequencies and amplitudes of limit cycles. In frequency domain analyses, a nonlinear transfer function between acoustic velocity and heat release rate perturbations, called the flame describing function (FDF), is obtained from a flame model or experiments. The FDF is a function of the frequency and amplitude of velocity perturbations but only contains the heat release response at the forcing frequency. This is based on the assumption that the response at higher harmonics is small compared to the response at the fundamental frequency and that the higher harmonics are filtered out by the system. While the gain and phase of the FDF provide insight into the nonlinear dynamics of the system, the accuracy of its predictions remains to be verified for different types of nonlinearity. In time domain analyses, the governing equations of the fully coupled problem are solved to find the time evolution of the system. One method is to use a Galerkin discretization for the acoustics. In our previous work we have shown that limit cycles predicted using the FDF are almost exactly the same as those obtained from the time-domain using only one Galerkin mode. We call this the single-mode method.
In this paper we compare results from the single-mode and multi-mode methods, applied to a thermoacoustic system of a premixed flame in a tube. Here 'mode' refers to a Galerkin mode. For some cases, the results differ greatly in both amplitude as well as frequency content. Furthermore, while the single-mode system always reaches a limit cycle, the multi-mode system shows more complex nonlinear behaviour such as multiple-periodicity. Multi-mode simulations show that the contribution from higher and subharmonics to the nonlinear dynamics can be significant and must be considered for an accurate and comprehensive analysis of thermoacoustic systems.

1. Introduction

Lean premixed combustion systems are susceptible to thermoacoustic instabilities, which occur due to the interaction between unsteady heat release rate and acoustic waves inside the combustor. Linear stability analysis of such systems can be used to predict frequencies and growth rates of linearly unstable modes. However, they can neither predict limit cycle amplitudes, nor a system's susceptibility to oscillations triggered by finite amplitude excitations.

Several studies have investigated nonlinear phenomena in combustion instabilities. In recent years, complex nonlinear phenomena such as triggering, hysteresis and mode-switching have been investigated experimentally and numerically [1, 2]. The analyses mentioned above use one of two types of approach: time domain or frequency domain. In the frequency domain approach based on the Flame Describing Function (FDF), quoting Noiray *et al.*, one assumes that the fundamental frequency determines the dynamics of the system while higher harmonics generated in the nonlinear processes are of sufficiently low amplitude to have negligible effect on the system's stability [1]. The FDF is then used in a nonlinear dispersion relation to calculate growth rates and frequencies as functions of perturbation amplitude. Their analysis highlights the importance of the amplitude-dependence of the gain and phase of the FDF on the nonlinear behaviour of the system. In the time domain approach the governing equations of the coupled problem are solved to compute the time evolution of the system. The time domain approach may be computationally expensive but it accounts for nonlinear interactions between modes and the influence of higher harmonics [3].

While the frequency domain approach has been successful in some practical systems, Subramanian *et al.* [4] argue that the system behaviour predicted using the FDF approach may be quantitatively as well as qualitatively different from that seen using time domain simulations of simple thermoacoustic models. They point out that using a two-part approach and a modal analysis fail to capture the intricate coupling between combustion and acoustics. In our previous work we have shown that the FDF approach yields the same results as the time domain approach with one Galerkin mode, but is different from that with several Galerkin modes [5].

The aims of this paper are to identify and explain the main differences between the single-mode and multi-mode methods for a few operating conditions of a simple thermoacoustic system of a premixed flame in a tube. Although the thermoacoustic system is simple, the fundamental nonlinear behaviour observed here is relevant to more complex thermoacoustic systems because the main source of nonlinearity is captured well.

2. Model for the acoustics

For the sake of simplicity, the acoustic chamber in the thermoacoustic system considered here is a duct of length L_0 open at both ends with a slot-stabilized 2-D laminar premixed flame located at a distance $\tilde{x}_f$ from one end. Fig. 1 shows a schematic. The base flow velocity is $\tilde{u}_0$, the pressure is $\tilde{p}_0$ and a constant mean density assumption is invoked so that the mean density, $\tilde{\rho}_0$, and speed of sound in the unburnt mixture, $\tilde{c}_0$, remain constant everywhere in the duct. The Mach number, $M \equiv \tilde{u}_0/\tilde{c}_0$, is assumed to be small and hence nonlinear effects in the acoustics are negligible [6]. A compact flame assumption is used here because the flame length is small compared to the wavelengths of the duct's acoustic modes. The dimensional governing equations for the acoustic perturbations are the momentum and energy equations:

$$\tilde{\rho}_0 \frac{\partial \tilde{u}}{\partial \tilde{t}} + \frac{\partial \tilde{p}}{\partial \tilde{x}} = 0; \quad \frac{\partial \tilde{p}}{\partial \tilde{t}} + \gamma \tilde{p}_0 \frac{\partial \tilde{u}}{\partial \tilde{x}} + \zeta \frac{\tilde{c}_0}{L_0} \tilde{p} - (\gamma - 1)\dot{\tilde{Q}}\delta(\tilde{x} - \tilde{x}_f) = 0 \tag{1}$$

where the rate of heat transfer from the flame to the gas is given by $\dot{\tilde{Q}}$, which is applied at the flame's position by multiplying $\dot{\tilde{Q}}$ by the dimensional Dirac delta distribution $\tilde{\delta}(\tilde{x} - \tilde{x}_f)$. The acoustic damping is represented by ζ and the model for this is described later.

The above equations may be non-dimensionalised using $\tilde{u}_0$, $\tilde{p}_0 \gamma M$, L_0 and $L_0/\tilde{c}_0$ for speed, pressure, length and time respectively. The dimensionless governing equations are:

$$\frac{\partial u}{\partial t} + \frac{\partial p}{\partial x} = 0; \quad \frac{\partial p}{\partial t} + \frac{\partial u}{\partial x} + \zeta p - \beta \dot{Q} \delta_D(x - x_f) = 0; \quad \beta \equiv \frac{(\gamma - 1)\dot{\tilde{Q}}_0 \alpha}{\gamma \tilde{p}_0 \tilde{u}_0}, \dot{Q} \equiv \frac{\dot{\tilde{Q}}}{\dot{\tilde{Q}}_0} \tag{2}$$

where $\beta\dot{Q}$ is the nondimensional heat release rate perturbation, which encapsulates all relevant information about the flame, base velocity and ambient conditions. The heat release rate is averaged over the cross-sectional area of the duct and the ratio of the area of base of the flame to the cross-sectional area of the duct, α, is assumed to be 0.05 in this paper.

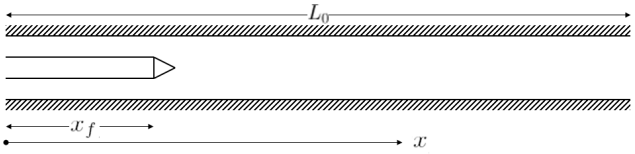

Figure 1. Schematic of the two-dimensional premixed flame in a duct. The flow is from left to right.

For the open duct examined here, the pressure perturbations and gradient of velocity perturbations are both set to zero at the ends of the tube.

$$[p]_{x=0} = [p]_{x=1} = 0; \quad \left[\frac{\partial u}{\partial x}\right]_{x=0} = \left[\frac{\partial u}{\partial x}\right]_{x=1} = 0. \tag{3}$$

These boundary conditions are enforced by choosing basis sets that match these boundary conditions and satisfy the dimensionless momentum equation:

$$u(x,t) = \sum_{j=1}^{N} \eta_j(t) cos(j\pi x); \quad p(x,t) = -\sum_{j=1}^{N} \frac{\dot{\eta}_j(t)}{j\pi} sin(j\pi x). \tag{4}$$

In this Galerkin discretization, all the basis vectors are orthogonal. The state of the system is given by the amplitudes of the Galerkin modes that represent velocity, η_j, and those that represent pressure, $\dot{\eta}_j$. The energy equation is discretized by substituting (4) into the dimensionless energy equation. The acoustic damping, ζ, is dealt with by assigning damping parameters, ζ_j, to each mode, where $\zeta_j = c_1 j^2 + c_2 j^{1/2}$. This model is based on correlations developed by Matveev [7]. It represents acoustic energy losses due to radiation from the open ends and dissipation in the acoustic viscous and thermal boundary layers at the duct walls. The dimensionless energy equation is then multiplied by $\sin(k\pi x)$ and integrated over the domain $x = [0, 1]$, thus reducing it to an ODE for each mode, *j*:

$$\frac{d}{dt}(\frac{\dot{\eta}_j}{j\pi}) + j\pi\eta_j + \zeta_j(\frac{\dot{\eta}_j}{j\pi}) + 2\beta sin(j\pi x_f) = 0, \tag{5}$$

which are integrated by direct time-marching from $t = 0$ using a first order Euler algorithm with a nondimensional time-step of 0.0005.

3. Model for the premixed flame

The flame is described by a kinematic model using a level set approach, also known as the *G*-equation model. Although this model is less complex than real premixed flames, it has been shown that it captures the major nonlinearities in premixed flame dynamics and is used widely in low-order models of thermoacoustic systems with premixed flames [6, 8].

The principal assumptions of the model are: (i) the flame is a thin surface separating unburnt reactants from burnt products; (ii) the influence of gas expansion across the flame front is negligible. Assumption (i) allows for the flame to be tracked using the *G*-equation (in two dimensions), as follows:

$$\frac{\partial G}{\partial \tilde{t}} + \tilde{U}\frac{\partial G}{\partial \tilde{x}} + \tilde{V}\frac{\partial G}{\partial \tilde{y}} = s_L\sqrt{\left(\frac{\partial G}{\partial \tilde{x}}\right)^2 + \left(\frac{\partial G}{\partial \tilde{y}}\right)^2} \tag{6}$$

where tildes denote dimensional values and *G(x,y,t)* is a time-varying function that takes negative values at points in the unburnt gas, positive values at points in the burnt gas and zero at points that lie on the flame surface. $\tilde{U}$ and $\tilde{V}$ are the instantaneous total velocities along the x and y directions. The flame speed, s_L, is a function of the equivalence ratio, but we only consider the dynamics of velocity perturbations imposed on fully premixed flames ignoring flame-stretch and curvature effects. Hence the equivalence ratio and flame speed are assumed to be uniform throughout the flow. Assumption (ii) allows for the velocity field to be independently specified, neglecting the coupling between the flow-field and flame surface evolution, and is the major simplifying assumption of this reduced order modelling approach.

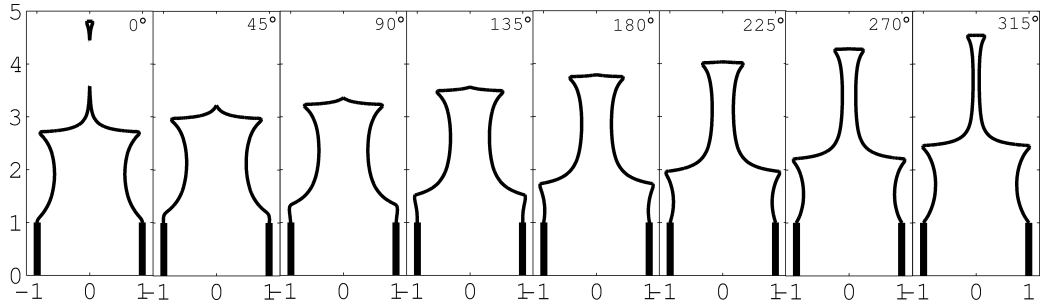

Figure 2. Instantaneous images of the flame during one cycle of a typical limit cycle oscillation, $\phi = 1.06$, $\beta_f = 2.14$, $\epsilon = 0.25$, $St = 1$, $K = 2.5$. Note the formation of sharp cusps towards the products, a distinct characteristic of premixed flames.

The acoustic velocity fluctuations at the base of the burner induce the roll up of vortices which distort the flame surface as they are convected downstream. Thus the axial perturbation in the flame domain can be modelled as a convective wave [8] and the nondimensional axial velocity field can be obtained from the time history of acoustic velocity fluctuations at the base of the burner. Within the flame domain, if the divergence free assumption is used for the hydrodynamics, the continuity equation can be solved to find the transverse velocity perturbation field, given an axial velocity perturbation field. Here we assume that $\epsilon = \tilde{u}/\tilde{u}_0$, the nondimensional velocity perturbation, remains constant as it is convected across the flame. The perturbation phase speed is not equal to the mean flow velocity but is obtained from direct numerical simulations as in Kashinath *et al.* [9]. Equation (6) is solved numerically as in Shreekrishna *et al.* [10].

Fig. 2 shows instantaneous flame images over one limit cycle oscillation. Here L_f is the nominal flame height, i.e. the height of the steady flame ignoring stretch effects, R is half-width of the burner and β_f is the flame aspect ratio, L_f/R.

For a premixed flame, the heat release rate can be written as an integral of local heat release rate contributions over the flame surface, which can be expressed in terms of *G* as an integral over the whole domain,

$$q(t) = \int_D \rho s_L(\phi) h_R(\phi) \left|\nabla G\right| \delta(G) dx^* dy^* \tag{7}$$

where, $\delta(G)$ is the Dirac-delta function and $h_R(\phi)$ is the heat of reaction. The above integral can be evaluated numerically using the formulation by Smereka [11]. Note that, for fully premixed flames with constant flame speed, heat release rate oscillations are only due to flame surface area fluctuations induced by velocity perturbations that distort the flame surface.

4. Comparison between single-mode and multi-mode simulations

In this section we compare time-domain simulations of the single-mode and multi-mode methods for three operating conditions. These operating conditions were chosen to highlight some of the

major differences between these two methods. While several different flame and acoustic parameters can be varied, we consider two important parameters in this study: (i) duct length; and (ii) flame position in the duct. The duct length alters the frequencies of the acoustic modes, which affects the flame response, while the flame position alters the phase between the unsteady flame and the acoustics, which affects the coupling between the two.

Fig. 3 compares the pressure and velocity traces, at the flame position $x_f = 0.1414$. It is clear

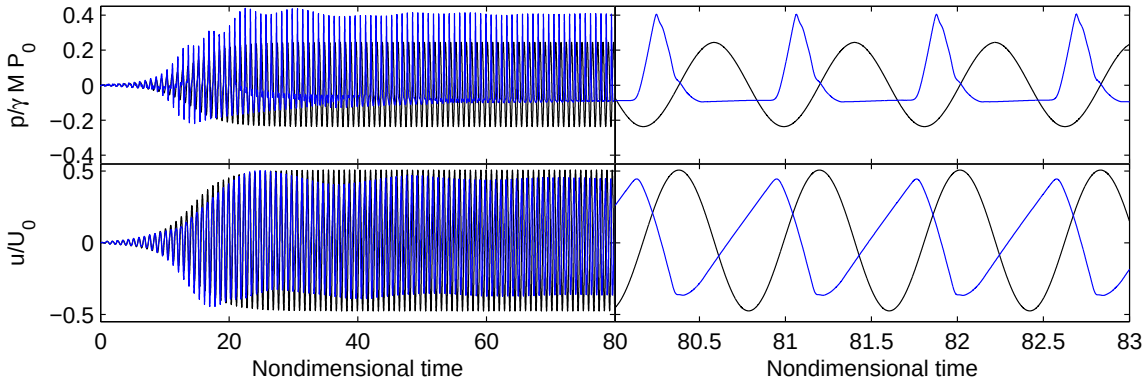

Figure 3. Time domain calculations for self-excited thermoacoustic systems with one mode (black) and twenty modes (blue): pressure and velocity traces, $f^* = \frac{c_0 L_f}{2u_0 L_0} = 1.2$, $K = 1.1$, $\beta_f = 7.0, \phi = 0.85$, $\zeta = 0.02$ $(c_1 = c_2 = 0.01)$, $x_f = 0.1414$

that there are some distinct differences between the two simulations. Firstly, while the single-mode pressure and velocity traces are symmetric about zero, there is a shift in the mean for the multi-mode case, especially noticeable in the pressure trace. Secondly, while the single-mode results are almost sinusoidal, the multi-mode results are far from sinusoidal, and once again, this is more noticeable in the pressure trace. Finally, the peak-to-peak values differ by about 20 percent. Fig. 4 compares the

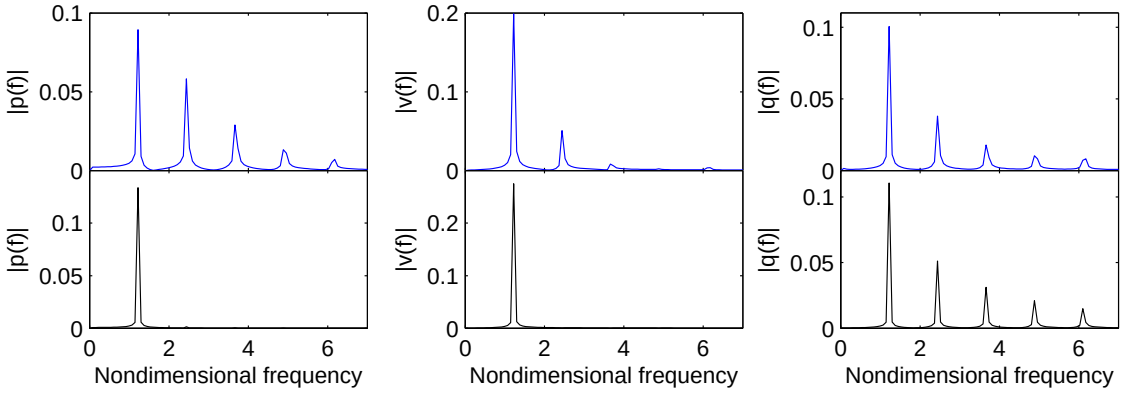

Figure 4. Pressure, velocity and heat release rate FFTs, $f^* = 1.2$, $K = 1.1$, $\beta_f = 7.0, \phi = 0.85$, $\zeta = 0.02$ $(c_1 = c_2 = 0.01)$, $x_f = 0.1414$

Fourier transforms of the pressure, velocity and heat release rate signals from the two simulations. While the heat release rate FFTs for the two are very similar and show a high degree of nonlinearity, the pressure and velocity FFTs are quite different. In the single-mode case there are no higher harmonics in pressure or velocity – the higher harmonics of the heat release rate cannot interact with the pressure or velocity perturbations because their contribution averages to zero over one cycle of the fundamental. In the multi-mode case, however, the higher harmonics of the heat release rate interact

with the higher Galerkin modes resulting in a remarkably different limit cycle, in terms of amplitude, frequency content and mode-shape.

Fig. 5 compares the pressure and heat release traces, at the flame position $x_f = 0.3586$, from the

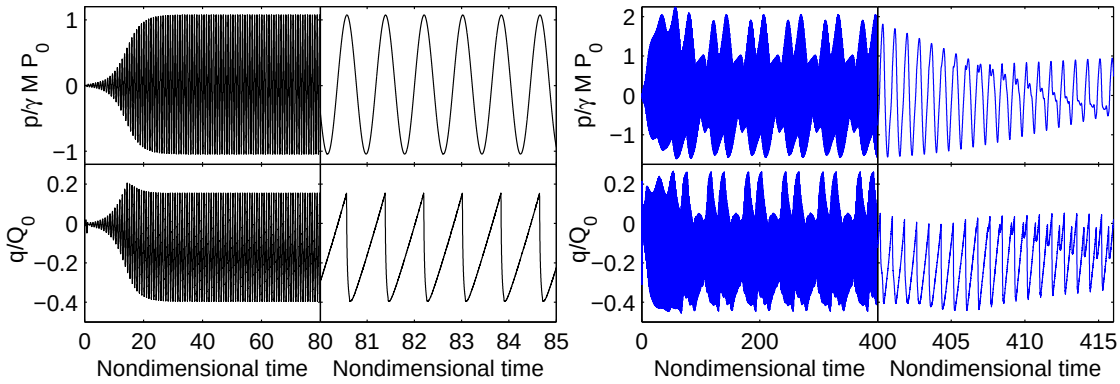

Figure 5. Time domain calculations for self-excited thermoacoustic systems with one mode (black) and twenty modes (blue): pressure and velocity traces, $f^* = \frac{c_0 L_f}{2u_0 L_0} = 1.2$, $K = 1.1$, $\beta_f = 7.0, \phi = 0.85$, $\zeta = 0.02$ $(c_1 = c_2 = 0.01)$, $x_f = 0.3586$

single-mode and multi-mode simulations. Note that this value for x_f is exactly $0.5 - x_f$ of the previous case. This position was chosen so that the coupling term in the energy equation, $(sin(j\pi x_f)cos(j\pi x_f))$, has the opposite sign to that of case-1 for all even harmonics. Since the heat release rate usually has a significant first harmonic, we expect this choice of flame position to result in very different nonlinear behaviour to case-1. The most striking difference between the single-mode and multi-mode simulations in Fig. 5 is that the multi-mode case does not have a limit cycle. While its behaviour is periodic, there are several frequencies, and in particular, some subharmonics are present. Secondly, the multi-mode time traces are highly asymmetric with the magnitudes of the peaks and troughs being quite different. Thirdly, at some instances, the peak-to-peak pressure of the multi-mode case can be upto 75 percent higher than that of the single-mode case. Fig. 6 compares the Fourier transforms

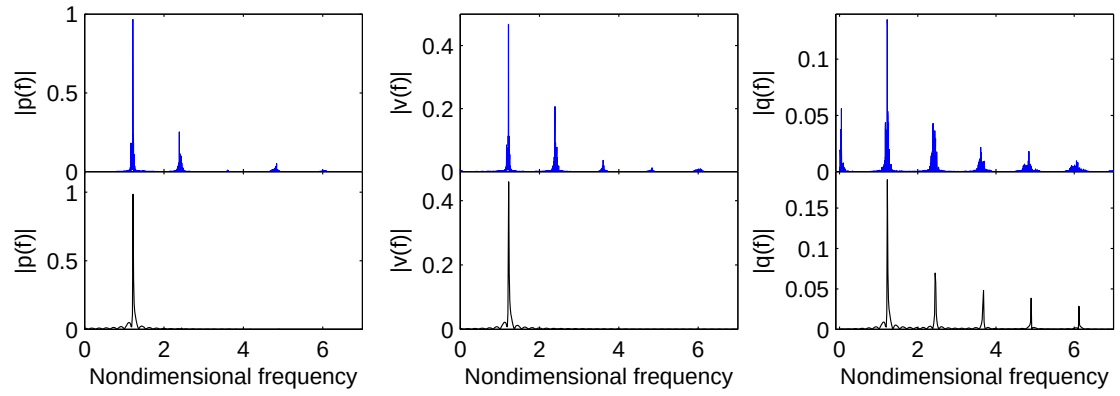

Figure 6. Pressure, velocity and heat release rate FFTs, $f^* = 1.2$, $K = 1.1$, $\beta_f = 7.0, \phi = 0.85$, $\zeta = 0.02$ $(c_1 = c_2 = 0.01)$, $x_f = 0.3586$

of the pressure, velocity and heat release rate signals from the two simulations. Unlike the previous case, the heat release rate FFTs for the single-mode and multi-mode simulations are not similar. The multi-mode heat release rate FFT has a distinct subharmonic with a period that is 32 times the fundamental. Also, besides having higher harmonics at multiples of the fundamental, the signal contains

other frequencies close to these harmonics. Just as in the previous case, the pressure and velocity FFTs are quite different; while the single-mode case has no higher harmonics, the multi-mode case contains higher harmonics.

Fig. 7 compares the pressure and velocity traces from the single-mode and multi-mode simulations,

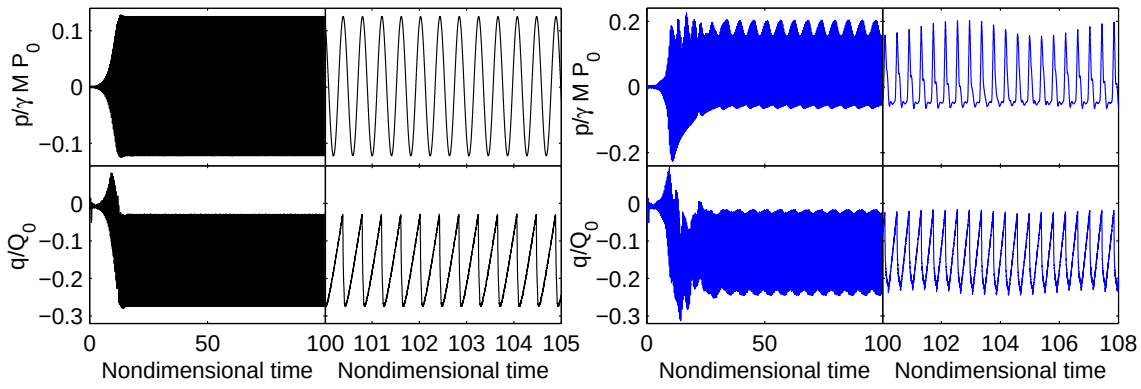

Figure 7. Time domain calculations for self-excited thermoacoustic systems with one mode (black) and twenty modes (blue): pressure and velocity traces, $f^* = \frac{c_0 L_f}{2u_0 L_0} = 2.4$, $K = 1.1$, $\beta_f = 7.0, \phi = 0.85$, $\zeta = 0.02$ $(c_1 = c_2 = 0.01)$, $x_f = 0.1414$

at the flame position $x_f = 0.1414$, with the duct length halved (i.e. f^* doubled). In this case, as in the previous one, the multi-mode simulation is periodic with several frequencies. Like in case-1, there is a shift in the mean pressure for the multi-mode case, and like in case-2, the trace is asymmetric about the mean. Fig. 8 compares the Fourier transforms. Similar to case-2, the multi-mode heat release rate

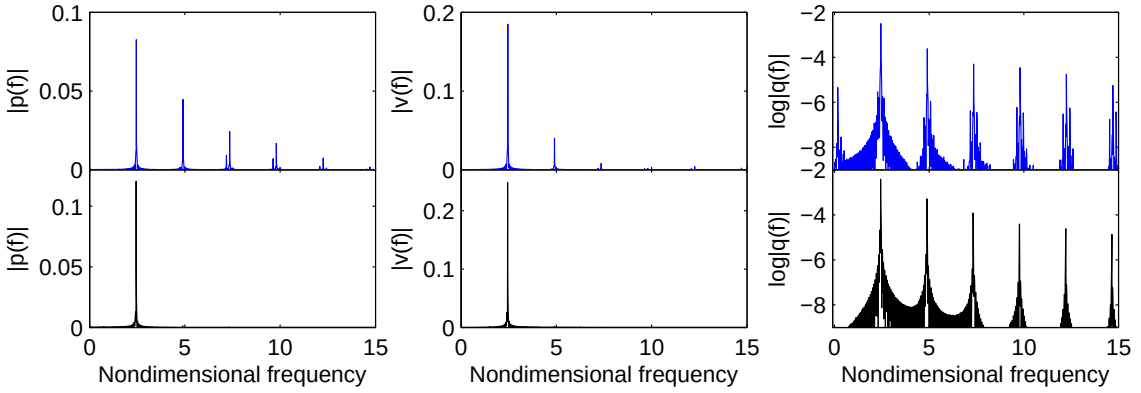

Figure 8. Pressure, velocity and heat release rate FFTs, $f^* = 2.4$, $K = 1.1$, $\beta_f = 7.0, \phi = 0.85$, $\zeta = 0.02$ $(c_1 = c_2 = 0.01)$, $x_f = 0.1414$

FFT has a subharmonic with a period that is 16 times the fundamental. The other characteristics are much like those in the previous two cases. The above three cases show that the single-mode simulations fail to capture the complex nonlinear phenomena that can be seen in the multi-mode simulations. They also show that, in some situations, the amplitude predicted by the single-mode simulation can be much smaller than that of the multi-mode simulation. The interactions between the higher harmonics and subharmonics of the heat release rate with those of the acoustics can lead to dramatically different nonlinear behaviour, which can not be captured using the single-mode approximation.

5. CONCLUSIONS

This paper compares predictions of nonlinear thermoacoustic phenomena of a simple premixed flame in a tube by single-mode and multi-mode time domain methods. It has been shown in previous work that frequency domain calculations using the flame describing function (FDF) are almost identical to time-domain calculations using a single Galerkin mode [5]. The flame is modelled using a nonlinear kinematic model based on the G-equation, while the acoustics are governed by linearised momentum and energy equations. The velocity field contains both axial and transverse velocity perturbations and the phase speed of convective disturbances is obtained from Kashinath *et al.* [9].

The single-mode simulations fail to capture the complex nonlinear phenomena that can be seen in the multi-mode simulations. In some situations, the amplitude predicted by the single-mode simulation is much smaller than that of the multi-mode simulation. In others, a shift in the mean pressure or velocity, asymmetric behaviour about the mean and the presence of subharmonics, which are seen in the multi-mode simulation can not be captured by the single-mode simulation. Although the heat release rate in the single-mode case can be highly nonlinear, because there is only a single acoustic mode, this does not affect the limit cycle amplitude. In the multi-mode case, however, the interactions between the higher harmonics and subharmonics of the heat release rate with those of the acoustics can lead to dramatically different nonlinear behaviour.

This study shows that, in some situations, the contribution from higher and sub-harmonics to the nonlinear dynamics can be significant and must be considered for an accurate and comprehensive analysis of thermoacoustic systems. A complete characterization of the bifurcation diagram is necessary to identify precisely the regions where the single-mode method is a good approximation and this requires fast matrix-free continuation, which will be the subject of future work.

REFERENCES

[1] Noiray, N., Durox, D., Schuller, T. and Candel, S. M., A unified framework for nonlinear combustion instability analysis based on the flame describing function, *J. Fluid Mech.,* **615**, 139–167, (2008).

[2] Moeck, J. P., Bothien, M. R., Schimek, S., Lacarelle, A., and Paschereit, C. O., Subcritical thermoacoustic instabilities in a premixed combustor, *14th AIAA/CEAS Aeroacoustics Conference,* 2008, Vancouver, Canada, 5–7 May, *AIAA 2008-2946.*

[3] Stow, S. R., and Dowling, A. P., A time-domain network model for nonlinear thermoacoustic oscillations, *ASME Turbo Expo,* 2008, Berlin, Germany, 9–13 June, *ASME GT2008-50770.*

[4] Subramanian, P., Gupta, V., Tulsyan, B., and Sujith, R. I., Can describing function technique predict bifurcations in thermoacoustic systems?, *16th AIAA/CEAS Aeroacoustics Conference,* 2010, Stockholm, Sweden, 7–9 June, *AIAA 2010-3860.*

[5] Kashinath, K., Hemchandra, S., and Juniper, M. P., Nonlinear phenomena in thermoacoustic systems with premixed flames, *ASME Turbo Expo,* 2012, Copenhagen, Denmark, 11–15 June, *ASME GT2012-68726.*

[6] Dowling, A. P., Nonlinear self-excited oscillations of a ducted flame, *J. Fluid Mech.,* **346**, 271–290, (1997).

[7] Matveev, I., *Thermo-acoustic instabilities in the Rijke tube: Experiments and modeling,* PhD thesis, CalTech., (2003).

[8] Schuller, T., Durox, D., and Candel, S., A unified model for the prediction of laminar flame transfer functions: comparisons between conical and v-flame dynamics, *Combust. Flame,* **134**, 21–34, (2003).

[9] Kashinath, K., Chawaliwong, K., Hemchandra, S., and Juniper, M. P., The effect of the phase speed of velocity perturbations on the nonlinear thermoacoustic behaviour of a ducted premixed flame, *Submitted to the Proceedings of the Combustion Institute,* 2012.

[10] Shreekrishna, Hemchandra, S., and Lieuwen, T., Premixed flame response to equivalence ratio perturbations, *Combust. Theor. amd Modelling,* **14**, 681–714, (2010).

[11] Smereka, P., The numerical approximation of a delta function with application to level set methods, *J. Comput. Phys.,* **211**, 77–90, (2006).